Original Article

Monte Carlo-based Investigation of Absorbed-dose Energy Dependence of Thermoluminescent Dosimeters in Therapeutic Proton and Carbon Ion Beams

Arghya Chattaraj[1,2], Subhalaxmi Mishra[1], T. Palani Selvam[1,2]

[1]Radiological Physics and Advisory Division, Health, Safety and Environment Group, Bhabha Atomic Research Centre, [2]Homi Bhabha National Institute, Mumbai, Maharashtra, India

Abstract

Background: The present study is aimed at calculating relative absorbed-dose energy response correction (*R*) of commonly used thermoluminescent dosimeters (TLDs) such as LiF, $Li_2B_4O_7$, and Al_2O_3 as a function of depth in water for protons (50–250 MeV/n) and carbon ion (80–480 MeV/n) beams using Monte Carlo-based FLUKA code. **Materials and Methods:** On-axis depth-dose profiles in water are calculated for protons (50–250 MeV/n) and carbon ion (80–480 MeV/n) beams using FLUKA code. For the calculation of *R*, selective depths are chosen based on the depth-dose profiles. In the simulations, the TLDs of dimensions 1 mm × 1 mm × 1 mm are positioned at the flat, dose gradient, and Bragg peak regions of the depth-dose profile. Absorbed dose to detector was calculated within the TLD material. In the second step, TLD voxels were replaced by water voxel of similar dimension and absorbed dose to water was scored. **Results:** The study reveals that for both proton and carbon ion beams, the value of *R* differs from unity significantly at the Bragg peak position and is close to unity at the flat region for the investigated TLDs. The calculated *R* value is sensitive to depth in water, beam energy, type of ion beam, and type of TLD. **Discussion:** For accurate dosimetry of protons and carbon ion beams using TLDs, the response of the TLD should be corrected to account for its absorbed-dose energy dependence.

Keywords: Carbon ions, Monte Carlo, protons, thermoluminescent dosimeter response

Received on: 07-02-2024 **Review completed on: 12-03-2024** **Accepted on: 17-03-2024** **Published on: 25-06-2024**

Introduction

Radiotherapy utilizing proton and carbon ion beams offers improved dose confirmation as compared to photons and electrons due to their capability to deliver high doses precisely at a well-defined depth (Bragg peak) and rapid dose falloff beyond the peak.[1,2] Various detectors, such as ionization chambers, silicon detectors, scintillation detectors, and thermoluminescent dosimeters (TLDs), are employed for dosimetry in this context.[3-15] Ionization chambers are often considered the most precise dosimeters and are commonly used for routine dosimetry. TLDs such as LiF, $Li_2B_4O_7$, and Al_2O_3 are employed for dose mapping and absolute dose measurements in radiation therapy, including proton and carbon ion beams.[8,16,17] The availability of TLDs in smaller dimensions and in various forms, such as powder, small extruded chips or ribbons, and thin Teflon-impregnated discs, makes the handling of these detectors relatively more convenient. In certain scenarios, TLDs are preferred over ionization chambers as they minimally perturb the radiation field. However, it is essential to note that the nonlinear dose-response curve of TLDs represents a limitation in proton and heavy-ion beam dosimetry.[5] This results in a dependence of the detector's response on the radiation beam quality and the particle's linear energy transfer (LET). Hence, special care is required when using TLDs in proton and heavy-ion beams to achieve a precision of ±3%.[18,19]

Address for correspondence: Mr. Arghya Chattaraj, Scientific Officer, Radiological Physics and Advisory Division, Health, Safety and Environment Group, Bhabha Atomic Research Centre, Mumbai - 400 085, Maharashtra, India.
E-mail: arghyac@barc.gov.in

Access this article online

Quick Response Code:

Website: www.jmp.org.in

DOI: 10.4103/jmp.jmp_25_24

How to cite this article: Chattaraj A, Mishra S, Selvam TP. Monte Carlo-based investigation of absorbed-dose energy dependence of thermoluminescent dosimeters in therapeutic proton and carbon ion beams. J Med Phys 2024;49:148-54.

Several studies have been conducted to examine the responses of various detectors in proton and heavy ion beams,[3-15] employing various approaches, including track structure theory, analytical algorithms, measurements, and Monte Carlo methods. McMahan[10] conducted measurements to assess the response of different scintillator detectors to ions with atomic numbers ranging from 1 to 84 and energies in the range of 5–30 MeV/n. Pereyra *et al*.[11] investigated the response of nuclear track detectors to energetic heavy ions, such as ^{4}He (150 MeV/n), ^{12}C (390 MeV/n), and ^{56}Fe (465 MeV/n), particularly in the relatively low-dose range of less than or equal to 1 mGy. Yasuda[14,15] conducted a study on the response of a direct ion storage dosimeter (DIS-1) when exposed to ^{4}He, ^{12}C, ^{40}Ar, and ^{56}Fe ion beams. Boscolo *et al*.[5] presented an analytical algorithm designed to calculate the relative thermoluminescence efficiency (TL-efficiency) with respect to ion charge (Z) and energy (E). Massillon-Jl *et al*.[9] irradiated LiF: Mg, Ti with ^{1}H (1, 3, 25, and 40 MeV),^{4}He (25 and 40 MeV/n), ^{12}C (15, 25, and 40 MeV/n), ^{16}O (25 MeV/n), and ^{20}Ne (40 MeV/n) to investigate the response of the TLD as a function of LET. The majority of the mentioned studies are based on measurements[3-15] and limited studies involved TLDs.[5,9]

Monte Carlo-based studies on the determination of energy dependence of TLDs such as LiF, $Li_2B_4O_7$, and Al_2O_3 TLDs in proton and carbon ion beams are not available in the literature. The energy dependence of a detector, such as TLDs in this case, is a product of its intrinsic energy dependence and the absorbed-dose energy dependence.[20-22] The intrinsic energy dependence relates the TLD light output to the dose received by the TLD for a given beam quality, and it cannot be calculated using Monte Carlo methods but can be determined through measurement. On the other hand, the absorbed-dose energy dependence of a detector relates the TLD response to the dose in the medium and can be calculated using Monte Carlo simulations. The present study is focused on determining the relative absorbed-dose energy response correction for commonly used TL detectors, namely LiF, $Li_2B_4O_7$, and Al_2O_3. This correction factor is calculated as a function of depth in a water phantom for nonmodulated proton (50–250 MeV/n) and carbon ion (80–480 MeV/n) beams. The investigation employs the Monte Carlo-based FLUKA code[23,24] for these calculations.

Materials and Methods

Ion beams and detectors

The present study considered (a) proton beams of energy ranging from 50 to 250 MeV/n (with an increment of 50 MeV/n), which correspond to the projected range of 2.2–37 g/cm^2 in water medium, and (b) carbon ion beams with energy ranging from 80 to 480 MeV/n (with varying intervals), which correspond to the projected range of 1.8–37 g/cm^2, in water medium. LiF, $Li_2B_4O_7$, and Al_2O_3 TLDs having dimension of 1 mm × 1 mm × 1 mm are considered in this study. Note that 1 mm x 1 mm x 1mm TLD cubes are commercially available. Elemental composition, mass fraction, effective atomic number (Z_{eff}), electron density (<*Z*/*A*>), and mass density (ρ) of these detectors are presented in Table 1.

Energy dependence of the detector

Absorbed-dose energy dependence, $f(Q)$, of a detector for a given beam quality Q is the ratio of the dose to the medium (water in the present study) at the point of measurement in the absence of the detector, D_{wat}, to the dose to the detector, D_{det}.[20-22] It can be written as:

$$f(Q) = \left[\frac{D_{wat}}{D_{det}}\right]_Q \quad (1)$$

The detectors are generally calibrated against a reference beam, which is ^{60}Co in the present study. Thus, for a given TLD and beam quality Q, relative absorbed-dose energy response correction factor R[20-22] can be written as:

$$R = \frac{\frac{1}{f(Q)}}{\frac{1}{f(Q_0)}} = \frac{\left[\frac{D_{det}}{D_{wat}}\right]_Q}{\left[\frac{D_{det}}{D_{wat}}\right]_{Q_0}} \quad (2)$$

where Q_0 is ^{60}Co beam in the present study. The beam quality, Q, denotes the proton and carbon ion beams of different energy.

FLUKA Monte Carlo code

Monte Carlo-based FLUKA code[23,24] (version 4.0, 2020) combined with FLAIR[25] (version 3.0.10) is used in the present study. Note that FLAIR is advanced graphical user interface for FLUKA. FLUKA is a general-purpose Monte Carlo code capable of transporting about 60 different particles in matter.[26] FLUKA is well benchmarked for the dosimetry of proton and carbon ions in the therapeutic energy range.[27,28] It has the capability to handle complex geometries using an improved version of the combinatorial geometry package. FLUKA treats elastic scattering through parameterized nucleon-nucleon cross sections and tabulated nucleon-nucleus cross sections. Inelastic cross sections for hadron-hadron interactions are represented by parameterized fits of the available experimental data. For hadron-nucleus interactions, a mixture of tabulated data and parameterized fits are used. The PEANUT package includes a very detailed generalized intranuclear cascade and a preequilibrium stage. This module is followed by equilibrium processes, evaporation, fission, Fermi breakup, and gamma de-excitation. Light residual nuclei are not evaporated but fragmented into a maximum of 6 bodies, according to a Fermi breakup model. Nuclear interactions generated by ions are treated through interfaces to external event generators. For example, modified Relativistic Quantum Molecular Dynamics (RQMD) is used between 0.1 and 5 GeV per nucleon. In the present study, RQMD-2.4 is linked by *ldpmqmd* script.

Monte Carlo calculations

The Monte Carlo simulations are carried out in two steps.

Step 1

A parallel ion beam of given kinetic energy (proton or carbon) having a field size of 5 cm × 5 cm is incident on the front surface of a cubical water phantom of dimensions 50 cm × 50 cm × 50 cm. The absorbed dose is calculated as a function of depth along the central axis in the water phantom using USRBIN scoring card. The voxel size used for scoring the absorbed dose is 2 mm × 2 mm × 0.25 mm. From the depth-dose profile, position of the Bragg peak for a given energy of ion beam (proton or carbon) is obtained. Percentage depth-dose (PDD) profile is calculated by normalizing the absorbed-dose value at each voxel with respect to the dose value at the Bragg peak position.

Step 2

Simulations are carried out to obtain detector-specific absorbed-dose energy response correction factor (R) at different depths along the central axis of the beam. The on-axis depths considered for proton beams above 50 MeV/n and carbon beams above 80 MeV/n are d_1 (Bragg peak position), d_2 (dose gradient region), and d_3 and d_4 (flat region), as shown in Figure 1. Because of smaller range of 50 MeV/n proton and 80 MeV/n carbon beams, depths considered are d_1 (Bragg peak position) and d_4 (flat region). The considered values of d_1, d_2, d_3, and d_4 for 50–250 MeV/n proton beams are shown in Table 2 and those for 80–480 MeV/n carbon ion beams are shown in Table 3. In the Monte Carlo simulations, cubical TL detectors (LiF or $Li_2B_4O_7$ or Al_2O_3) of dimensions 1 mm × 1 mm × 1 mm are positioned at the above-described depths in the water phantom. Absorbed dose to detector (D_{det}) is scored on a region basis using USRBIN scoring card. Similar simulation is carried out to obtain absorbed dose to water (D_{wat}) by replacing the detector material as water. Note that for a given beam, placing of TLDs at all the depths in a single simulation will alter the water-equivalent depth of calculation which will affect the calculated value of R. Hence, in the present study, for a given beam, separate simulation was carried out for each investigated depth in water. Detector-to-water dose ratio for a given beam quality Q (numerator of equation 2) was calculated by taking the ratio of D_{det} and D_{wat}. The value of $\frac{1}{f(Q_0)} = \left[\frac{D_{det}}{D_{med}}\right]_{Q_0}$ (denominator of equation 2) is taken from a previously published study[29] for LiF, $Li_2B_4O_7$, and Al_2O_3 detectors. It was demonstrated by Selvam and Keshavkumar[30] that the detector-to-water dose ratio calculated for ^{60}Co beam in water phantom is independent of detector thickness ranging from 0.1 to 5 mm.

In the Monte Carlo calculations, PRECISIOn default card was used where both particle transport threshold and delta-ray production threshold were set at 100 keV. EVAPORAT and COALESCE PHYSICS cards were activated. Total 10^8 primary particles were simulated to achieve 1 σ level statistical uncertainty in absorbed dose below 1%. As per the recommendations of AAPM Task Group 268,[31] Table 4 summarizes all the Monte Carlo parameters used in this study.

Results and Discussion

Analysis of percentage depth dose

PDDs for the investigated energies of proton and carbon ion beams for field size of 5 cm × 5 cm are presented in Figures 2 and 3, respectively. The positions of the Bragg peaks in the water phantom for proton beams of energies 50, 100, 150, 200, and 250 MeV/n are at 2.1, 7.6, 15.6, 25.6, and 37.6 cm, respectively. Similarly, for carbon ion beams of energies 80, 130, 200, 300, 400, and 480 MeV/n, Bragg peaks occur at depths of 1.6, 4.1, 8.6, 17.1, 27.3, and 36.3 cm, respectively. The positions of the Bragg peaks are consistent with the calculated projected range of the proton and carbon ion beams in water using SRIM code.[32] In the depth-dose profiles of protons and carbon ions, as shown in Figures 2 and 3: (a)

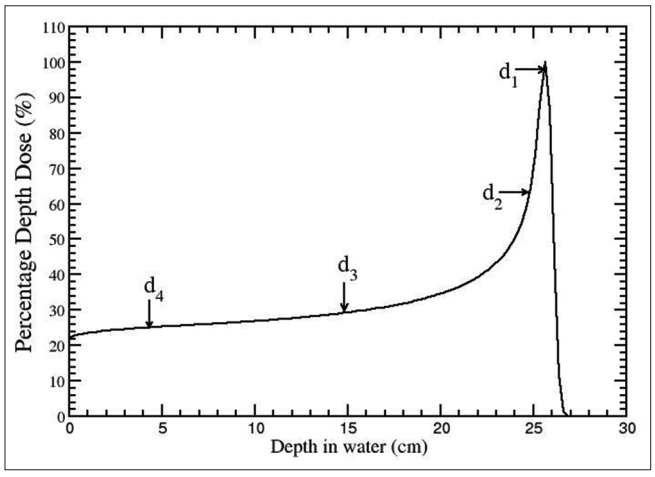

Figure 1: Schematic depiction of the positions of thermoluminescent dosimeters (d_1-d_4) on the depth-dose profile. d_1 represents Bragg peak, d_2 represents dose gradient region, and d_3-d_4 represent flat region of the depth-dose profile

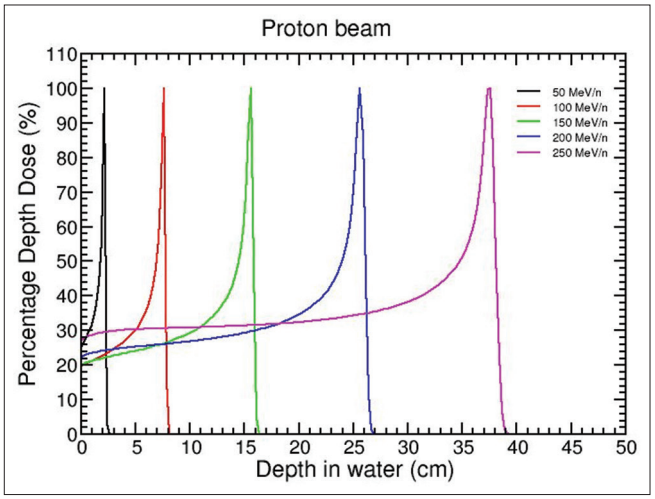

Figure 2: FLUKA-calculated percentage depth-dose profiles of the investigated energies of proton beams in water for a field size of 5 cm × 5 cm

Table 1: Elemental composition, mass fraction, effective atomic number (Z_{eff}), electron density (<Z/A>), and mass density (ρ) of LiF, $Li_2B_4O_7$, and Al_2O_3 detectors

Detector	H	Li	B	O	F	Al	Z_{eff}	<Z/A> (mol/g)	ρ (g/cm³)
LiF	-	0.268	-	-	0.732	-	8.27	0.462	2.635
$Li_2B_4O_7$	-	0.082	0.257	0.661	-	-	7.4	0.485	2.44
Al_2O_3	-	-	-	0.471	-	0.529	10.2	0.491	3.97
H_2O	0.112	-	-	0.888	-	-	7.4	0.555	1

Table 2: On-axis depths in water considered for the calculation of R of LiF, Li_2B_4O7, and Al_2O_3 detectors for monoenergetic proton beams

E (MeV/n)	d_1 (cm)	d_2 (cm)	d_3 (cm)	d_4 (cm)
50	2.125	-	-	1.125
100	7.625	6.625	5.0	3.0
150	15.625	14.625	10.0	5.0
200	25.625	24.625	20	10
250	37.625	36.625	20	10

Table 3: On-axis depths in water considered for the calculation of R of LiF, $Li_2B_4O_7$, and Al_2O_3 detectors for monoenergetic carbon ion beams

E (MeV/n)	d_1 (cm)	d_2 (cm)	d_3 (cm)	d_4 (cm)
80	1.625	-	-	0.625
130	4.125	3.625	2.625	0.625
200	8.625	8.375	4.625	0.625
300	17.125	16.625	8.875	0.625
400	27.375	26.875	13.875	0.625
480	36.375	35.875	18.125	0.625

rapid dose falloff is observed beyond the Bragg peak region for protons and (b) in the case of carbon ions, a tail is observed beyond the Bragg peak region of the depth-dose profile and the magnitude of this tail part increases with increase in carbon ion beam energy. As an example, for 80 MeV/n, 200 MeV/n, and 480 MeV/n carbon ion beams, beyond few mm of the Bragg peak positions, doses fall down to about 1%, 5%, and 17% of the peak dose, respectively. This is because primary carbon ions undergo nuclear interactions and fragment into lower atomic number particles such as protons and alpha producing a fragmentation tail beyond the Bragg peak.[33-35]

Relative absorbed-dose energy response correction

The Monte Carlo-calculated values of *R* for LiF, $Li_2B_4O_7$, and Al_2O_3 detectors are presented in Tables 5 and 6 for depths d_1-d_4 in water phantom for proton and carbon beams, respectively. For a given detector, *R* values are independent of energy of the proton beams at the depths, d_2-d_4, in the water phantom. At these depths (d_2-d_4), *R* values are close to unity for LiF and $Li_2B_4O_7$ detectors. However, for Al_2O_3 detector at depths (d_2-d_4), *R* values are about 6%–9% lesser than unity depending on the beam energy and detector position. At the Bragg peak (d_1), *R* is sensitive to the energy of proton beam and the type of detector. For example, depending on kinetic energy

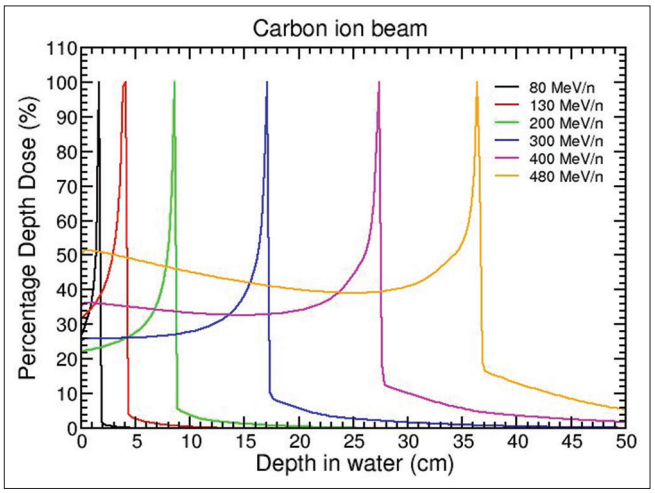

Figure 3: FLUKA-calculated percentage depth-dose profiles of the investigated energies of carbon ion beams in water for a field size of 5 cm × 5 cm

of proton beams, the value of *R* at the Bragg peak positions ranges from 0.817 to 0.971, 0.824 to 0.955, and 0.565 to 0.858 for LiF, $Li_2B_4O_7$, and Al_2O_3 detectors, respectively. Note that at a given energy of proton beam and depth in water, the values of *R* are comparable for LiF and $Li_2B_4O_7$ detectors (within 2%).

R values for carbon ion beams follow a similar trend as that of proton beams. For example, for LiF and $Li_2B_4O_7$ detectors, *R* values are close to unity (within 5%) at depths d_2-d_4 for all the investigated energies of Carbon ion. Whereas, in the case of Al_2O_3, the maximum deviation of *R* from unity is about 10% for 300 MeV/n at d_3 depth. However, at d_1, depending on the energy of the carbon ion beam, *R* values lie in the range of (a) 0.484–1.092 for LiF, (b) 0.489–1.147 for $Li_2B_4O_7$, and (c) 0.309–0.924 for Al_2O_3 detector.

Note that for a given energy of proton or carbon ion beam, R depends on the detector-to-water dose ratio (numerator of equation 2) and the detector-to-water dose ratio at reference beam, ^{60}Co (denominator of equation 2). For a given detector, $\left[\frac{D_{det}}{D_{wat}}\right]_{Q_0}$ is independent of depth in the water. For example, $\left[\frac{D_{det}}{D_{wat}}\right]_{Q_0}$ = 0.833, 0.873, and 0.882 respectively, for LiF, $Li_2B_4O_7$, and Al_2O_3 detectors.[29] This is because at ^{60}Co energies, the interaction mechanism of photons with water

or detector material at various depths is predominantly by Compton scattering and therefore energy transferred to secondary electrons is proportional to electron density. In the case of ion beams, significant difference in the values of $\left[\frac{D_{det}}{D_{wat}}\right]$ is observed as a function of depth in water. Hence, R values of a given energy (Q) of ion beam mostly follow the behavior of $\left[\frac{D_{det}}{D_{wat}}\right]_Q$. Variation in $\left[\frac{D_{det}}{D_{wat}}\right]_Q$ with depth in water and energy of the ion beam is due to the contributions from primary ion beam as well as secondaries generated. However, secondaries such as deuterons and other heavier ions collectively comprise about 1% or less of the total absorbed dose[33,36] and hence have least importance in dosimetry. Thus, $\left[\frac{D_{det}}{D_{wat}}\right]_Q$ value depends mostly on the energy deposited by the primary particles through ionization process.

Electronic mass collision stopping power $(S/\rho)_e$ values play a major role in the determination of $\left[\frac{D_{det}}{D_{wat}}\right]_Q$. For better understanding of the results, calculations of $(S/\rho)_e$ in water as a function of kinetic energy of protons and carbon ions are carried out using SRIM code.[32] Figures 4 and 5 present the ratio of $(S/\rho)_e$ of the investigated TLD materials to that of water as a function of kinetic energy of proton and carbon ion beams, respectively. For example, $(S/\rho)_e$ in water varies in the range of 12.6–3.95 MeV-cm^2/g and 298–98.5 MeV-cm^2/g for proton beams of energy 50–250 MeV/n and carbon beams of energy 80-480 MeV/n, respectively.[32] As the depth increases, kinetic energy of the beam decreases and therefore $(S/\rho)_e$ increases with depth. It is observed that $\left[\frac{D_{det}}{D_{wat}}\right]_Q$ compares well with the detector-to-water ratio of $(S/\rho)_e$ with a maximum deviation of 4% at the flat region (depths d_2 and d_4). However, at Bragg peak, $\left[\frac{D_{det}}{D_{wat}}\right]_Q$ does not follow the detector-to-water $(S/\rho)_e$ ratio. The variation of R with depth can be explained as follows:

At depths d_2-d_4

values of $\left[\frac{D_{det}}{D_{wat}}\right]_Q$ for a given energy of ion beams are comparable to detector-to-water ratio of $(S/\rho)_e$. This is because at these depths the particle (proton or carbon ion) has sufficient kinetic energy to cross the 1 mm-thick TLD voxel by depositing energy which is dictated by $(S/\rho)_e$ of the detector material. As calculated using SRIM code,[32] the minimum kinetic energy required to cross 1 mm thick water, LiF, $Li_2B_4O_7$, and Al_2O_3 voxel are 9, 14, 14, and 17 MeV/n, respectively, for protons. Similarly, these values of kinetic energy for carbon ions are 17, 25, 24, and 31 MeV/n, respectively. Note that the kinetic energy of the primary particles (protons and carbons) is greater than the minimum required energy to cross the TLD voxel. A difference of about 3% between the values of $\left[\frac{D_{det}}{D_{wat}}\right]_Q$ and detector-to-water ratio of $(S/\rho)_e$ may be mainly due to the associated statistical uncertainties on the calculated $\left[\frac{D_{det}}{D_{wat}}\right]_Q$ values which is about 1.5%.

At d_1 depth (Bragg peak)

For a given energy of proton or carbon ion beams, kinetic energy of the incident ion beam decreases at Bragg peak significantly. As a result, the particles will not have sufficient kinetic energy to cross the TLD voxel and stop within the voxel depositing their entire energy, and hence, $\left[\frac{D_{det}}{D_{wat}}\right]_Q$ does not follow detector-to-water ratio of $(S/\rho)_e$.

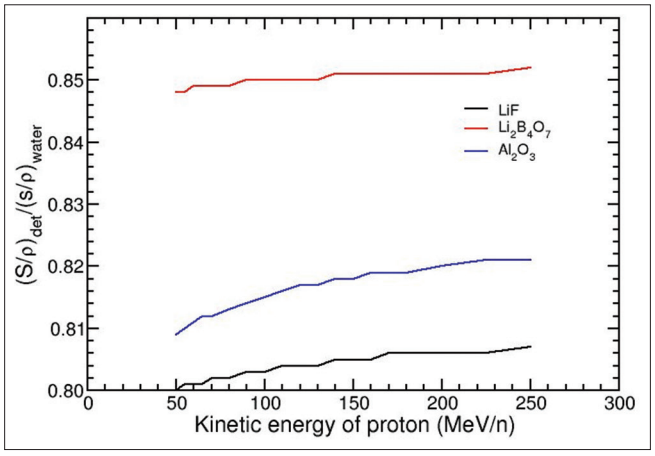

Figure 4: SRIM[32] calculated ratio of electronic mass stopping power of LiF, $Li_2B_4O_7$, and Al_2O_3 thermoluminescent dosimeter materials to water as a function of kinetic energy of protons

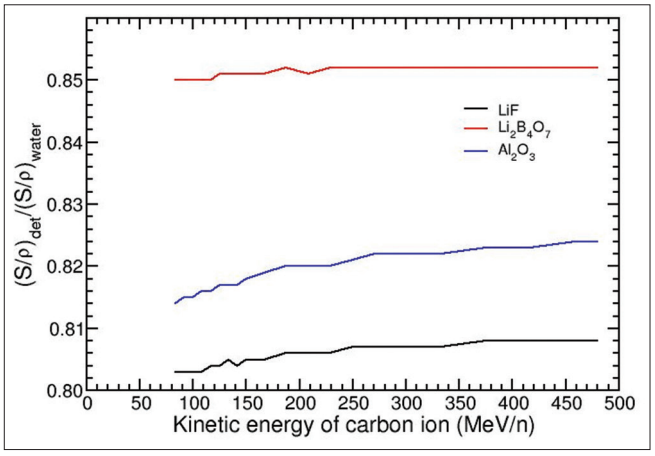

Figure 5: SRIM[32] calculated ratio of electronic mass stopping power of LiF, $Li_2B_4O_7$, and Al_2O_3 thermoluminescent dosimeter materials to water as a function of kinetic energy of carbon ions

Table 4: Summary of parameters used for Monte Carlo calculations as per the recommendations of AAPM Task Group-286[31]

Item name	Descriptions	References
Code, version/release date	FLUKA code (version 4.0)/26.11.2020	[23,24]
Validation	Validated for high-energy proton and carbon ion beams for medical applications	[26,27]
Timing	About 2160 total CPU hours on Intel (R) Xeon (R) 15 CPUs with clock speeds of 2.6 GHz	
Source description	Nonmodulated proton beam energy ranges from 50 to 250 MeV/n (with an increment of 50 MeV)	
	Nonmodulated carbon beam energy ranges from 80 to 480 MeV/n (with varying intervals)	
Cross sections	Elastic scattering through parameterized nucleon-nucleon cross sections and tabulated nucleon-nucleus cross sections	
	Inelastic scattering for hadron-hadron interactions is from parameterized fits of the available experimental data. For hadron-nucleus interactions a mixture of tabulated data and parameterized fits are used	
Transport parameters	PRECISIOn default card is used where both the particle transport threshold and delta-ray production threshold are set at 100 keV. EVAPORAT and COALESCE PHYSICS cards are activated. RQMD-2.4 is linked by *ldpmqmd* script	
VRT and AEIT	No variance reduction technique is used in this study	
Scored quantities	Dose to detector is scored using USRBIN card	
Number of histories/ statistical uncertainties	Up to 10^8 histories are simulated/1σ statistical uncertainties on the calculated values are <1%	
Statistical methods	Uncertainties are calculated with the default history-by-history method	
Postprocessing	Results are reported without using any kind of filtration	

CPU: Central processing unit, RQMD: Relativistic Quantum Molecular Dynamics, VRT: Variance Reduction Technique, USRBIN: Expansion not required. It is technical term of FLUKA Monte Carlo code, AAPM: American Association of Physicists in Medicine, AEIT: Approximate Efficiency Improvement Technique

Table 5: Relative absorbed-dose energy response correction, *R*, presented for LiF, $Li_2B_4O_7$, and Al_2O_3 detectors for proton beams at different depths in the water phantom

Energy (MeV/n)	LiF				$Li_2B_4O_7$				Al_2O_3			
	d_1	d_2	d_3	d_4	d_1	d_2	d_3	d_4	d_1	d_2	d_3	d_4
50	0.926	-	-	1.004	0.949	-	-	0.992	0.592	-	-	0.942
100	0.817	1.010	0.990	0.991	0.824	1.004	0.983	0.985	0.565	0.939	0.908	0.929
150	0.905	1.013	0.992	0.997	0.903	1.001	0.982	0.985	0.730	0.942	0.913	0.924
200	0.971	1.003	0.988	1.007	0.955	0.989	0.980	0.991	0.858	0.937	0.913	0.929
250	0.948	1.013	1.006	1.005	0.937	0.992	0.992	0.998	0.830	0.942	0.927	0.930

Table 6: Relative absorbed-dose energy response correction, *R*, presented for LiF, $Li_2B_4O_7$, and Al_2O_3 detectors for carbon ion beams at different depths in the water phantom

Energy (MeV/n)	LiF				$Li_2B_4O_7$				Al_2O_3			
	d_1	d_2	d_3	d_4	d_1	d_2	d_3	d_4	d_1	d_2	d_3	d_4
80	1.092	-	-	1.030	1.147	-	-	1.008	0.705	-	-	0.969
130	0.484	1.011	1.003	1.013	0.489	1.009	0.984	0.976	0.309	1.000	0.971	0.940
200	0.512	1.055	0.984	0.989	0.590	1.054	0.961	0.970	0.370	1.054	0.917	0.931
300	0.643	1.045	0.956	1.005	0.661	1.024	0.979	1.002	0.427	1.013	0.898	0.940
400	0.604	1.017	0.975	0.991	0.764	0.997	0.977	0.962	0.508	1.007	0.914	0.930
480	1.059	1.022	1.007	0.972	1.038	1.004	1.021	0.960	0.924	0.994	0.947	0.936

The width of the Bragg peak for monoenergetic ion beams is so narrow that it may be considered to occur at a point, and due to the positioning of high density 1 mm thick TLD, the position of the Bragg peak will be shifted toward the smaller depth (as compared to position in water). As a result of this, a portion of TLD will lie at the distal end of the Bragg peak where kinetic energy of the residual particles (protons or carbon ions) is less as compared to the remaining portion of TLD. However, when the TLD is replaced with water medium, this effect is not significant.

For investigating the effect of TLD thickness on the calculated R values, auxiliary simulations were carried out for Al_2O_3 TLD of thickness 0.1 mm placed at the Bragg peak locations of 50 and 250 MeV/n protons as well as 80 and 480 MeV/n carbon ions. The R values obtained for 0.1 mm thick Al_2O_3 TLD are: (a) 0.922 and 0.879 for 50 and 250 MeV/n protons, respectively, and (b) 0.941 and 0.907 for 80 and 480 MeV/n carbon ions, respectively. Thus, for thin detector positioned at the Bragg peak location, R approaches unity when the energy of the ion is smaller (for example, 50 MeV/n proton and 80 MeV/n carbon ions). Whereas,

for high energy ions (for example, 250 MeV/n proton and 480 MeV/n carbon ions), the response is less sensitive to the thickness of TLD. This suggests the importance of establishing detector thickness-specific R values for the ion beams.

Conclusion

The present study calculated *R* values for LiF, $Li_2B_4O_7$, and Al_2O_3 detectors as a function of depth in water for 5 cm × 5 cm nonmodulated proton (50–250 MeV/n) and carbon ion (80–480 MeV/n) beams using FLUKA Monte Carlo code. This study shows that the calculated *R* values for LiF, $Li_2B_4O_7$, and Al_2O_3 detectors are insensitive to depth in water in the flat region of depth-dose profile and sensitive in the dose gradient region including at Bragg peak. The study also reveals that, for both the proton and carbon ion beams, the values of *R* differ from unity significantly at the Bragg peak position (d_1) and the degree of deviation from unity depends on the energy, type of ion beam, type of detector, and its thickness. The values of *R* are close to unity (maximum deviation of about 7% for Al_2O_3 detector) at the flat region for the investigated detectors. The degree of deviation of R from unity reduces for thinner detector when the beam energy is smaller. The study suggests that for accurate dosimetry of protons and carbon ion beams using TLDs, the response of the TLD should be corrected to account for the beam-specific absorbed-dose energy dependence.

Financial support and sponsorship

Nil.

Conflicts of interest

There are no conflicts of interest.

References

1. Jäkel O, Schulz-Ertner D, Karger CP, Nikoghosyan A, Debus J. Heavy ion therapy: Status and perspectives. Technol Cancer Res Treat 2003;2:377-87.
2. Kato T. Current status of dosimetry tools for clinical proton beams. Radiat Environ Med 2019;8:59-69.
3. Bahl S, Lochab S, Aleynikov V, Molokanov A, Rupasov A, Pandey A, *et al.* Thermoluminescent response of nanocrystalline Ba0.97Ca 0.03SO4: Eu for proton beam. Indian J Pure Appl Phys 2010;48:500-4.
4. Berger T, Hajek M. On the linearity of the high-temperature emission from 7LiF: Mg, Ti (TLD-700). Radiat Meas 2008;43:1467-73.
5. Boscolo D, Scifoni E, Carlino A, La Tessa C, Berger T, Durante M, *et al.* TLD efficiency calculations for heavy ions: An analytical approach. Eur Phys J D 2015;69:1-6.
6. Boscolo D, Scognamiglio D, Horst F, Weber U, Schuy C, Durante M, *et al.* Characterization of the secondary neutron field produced in a thick aluminum shield by 1 GeV/u 56Fe ions using TLD-based ambient dosimeters. Front Phys 2020;8:365.
7. D'Avino V, Tommasino F, Lorentini S, La Verde G, Pugliese M. The performance of LiF: Mg-Ti for proton dosimetry within the framework of the MoVe IT project. ApplSci 2021;11:8263.
8. Geiß O, Krämer M, Kraft G. Efficiency of thermoluminescent detectors to heavy charged particles. Nucl Instrum Methods Phys Research B Beam Interact Mater Atoms 1998;142:592-8.
9. Massillon-Jl G, Gamboa-deBuen I, Brandan M. TL response of LiF: Mg, Ti exposed to intermediate energy 1H, 3He, 12C, 16O and 20Ne ions. J Phys D Appl Phys 2007;40:2584.
10. McMahan M. The response of scintillators to heavy ions-I. Plastics. IEEE Trans Nucl Sci 1988;35:42-6.
11. Pereyra P, López Herrera M, Palacios D, Viloria T, Vadillo E, Pérez B, *et al.* Nuclear track detector response to energetic heavy ions: Study Case. J Radioanal Nucl Chem 2020;324:609-14.
12. Shirazi A, Mahdavi SR, Khodadadee A, Ghaffory M, Mesbahi A. Monte Carlo simulation of TLD response function: Scattered radiation field application. Rep Pract Oncol Radiother 2008;13:23-8.
13. Weijers T, Davies J, Elliman R, Ophel T, Timmers H. Silicon detector response to heavy ions at energies of 1–2 MeV/amu. Nucl Instrum Methods Phys Res B Beam Interact Mater Atoms 2002;190:387-92.
14. Yasuda H. Responses of a direct ion storage dosimeter (DIS-1) to heavy charged particles. Radiat Res 2001;156:805-8.
15. Yasuda H, Fujitaka K. Responses of TLD-BeO: Na (UD-170A) to heavy ions and space radiation. Radiat Prot Dosimetry 2001;94:275-80.
16. Karger CP, Jäkel O, Palmans H, Kanai T. Dosimetry for ion beam radiotherapy. Phys Med Biol 2010;55:R193-234.
17. Rossomme S, Marinelli M, Verona-Rinati G, Romano F, Cirrone PA, Kacperek A, *et al.* Response of synthetic diamond detectors in proton, carbon, and oxygen ion beams. Med Phys 2017;44:5445-9.
18. Chu S, Bjorkholm JE, Ashkin A, Cable A. Experimental observation of optically trapped atoms. Phys Rev Lett 1986;57:314-7.
19. Tochilin E, Goldstein N, Lyman J, Miller W. The Quality and Let Dependence of Three Thermoluminescent Dosimeters and Their Potential use as Secondary Standards. San Francisco, Calif: Naval Radiological Defense Laboratory; 1968.
20. DeWerd L, Bartol L, Davis S. Thermoluminescence dosimetry. In: Clinical Dosimetry Measurements in Radiotherapy. Madison WI: Medical Physics Publishing; 2009.
21. Rogers D. General characteristics of radiation dosimeters and a terminology to describe them. In: Clinical Dosimetry Measurements in Radiotherapy. Madison WI: Medical Physics Publishing; 2009. p. 137-46.
22. Sutherland JG, Rogers DW. Monte Carlo calculated absorbed-dose energy dependence of EBT and EBT2 film. Med Phys 2010;37:1110-6.
23. Battistoni G, Boehlen T, Cerutti F, Chin PW, Esposito LS, Fassò A, *et al.* Overview of the FLUKA code. Ann Nucl Energy 2015;82:10-8.
24. Böhlen T, Cerutti F, Chin M, Fassò A, Ferrari A, Ortega PG, *et al.* The FLUKA code: Developments and challenges for high energy and medical applications. Nucl Data Sheets 2014;120:211-4.
25. Vlachoudis V. FLAIR: A Powerful But User Friendly Graphical Interface for FLUKA. Proc Int Conf on Mathematics, Computational Methods & Reactor Physics (M&C 2009), Saratoga Springs, New York; 2009.
26. Ballarini F, Battistoni G, Cerutti F, Empl A, Fasso A, Ferrari A, *et al.* Nuclear models in FLUKA: Present Capabilities, open problems, and future improvements. AIP Conf Proc 2005;769:1197-202.
27. Battistoni G, Bauer J, Boehlen TT, Cerutti F, Chin MP, Dos Santos Augusto R, *et al.* The FLUKA code: An accurate simulation tool for particle therapy. Front Oncol 2016;6:116.
28. Kozłowska WS, Böhlen TT, Cuccagna C, Ferrari A, Fracchiolla F, Magro G, *et al.* FLUKA particle therapy tool for Monte Carlo independent calculation of scanned proton and carbon ion beam therapy. Phys Med Biol 2019;64:075012-13.
29. Subhalaxmi M, Selvam TP. Monte Carlo-based beam quality and phantom scatter corrections for solid-state detectors in 60Co and 192Ir brachytherapy dosimetry. J Appl Clin Med Phys 2014;15:4907.
30. Selvam TP, Keshavkumar B. Monte Carlo investigation of energy response of various detector materials in ^{125}I and ^{169}Yb brachytherapy dosimetry. J Appl Clin Med Phys 2010;11:3282.
31. Sechopoulos I, Rogers DW, Bazalova-Carter M, Bolch WE, Heath EC, McNitt-Gray MF, *et al.* RECORDS: Improved reporting of montE CarlO RaDiation transport studies: Report of the AAPM research committee task group 268. Med Phys 2018;45:e1-5.
32. Ziegler JF, Ziegler MD, Biersack JP. SRIM–The stopping and range of ions in matter (2010). Nucl Instrum Methods Phys Res Beam Interact Mater Atoms 2010;268:1818-23.
33. Jäkel O. Physical advantages of particles: Protons and light ions. Br J Radiol 2020;93:20190428-37.
34. Mohamad O, Sishc BJ, Saha J, Pompos A, Rahimi A, Story MD, *et al.* Carbon ion radiotherapy: A review of clinical experiences and preclinical research, with an emphasis on DNA damage/repair. Cancers (Basel) 2017;9:66.
35. Ohno T. Particle radiotherapy with carbon ion beams. EPMA J 2013;4:9.
36. Newhauser WD, Zhang R. The physics of proton therapy. Phys Med Biol 2015;60:R155-209.